2 MRI and Functional MRI

Erin D. Bigler[1,2], Mark Allen[1] and Gary K. Stimac[3]

[1]*Psychology Department and The Neuroscience Center, Brigham Young University, Utah, USA*
[2]*Department of Psychiatry, University of Utah, Salt Lake City, Utah, USA*
[3]*Diagnostic Radiologist, Bellevue, WA, USA*

Neuroimaging provides objective findings that demonstrate the anatomical and functional status of the brain. In a forensic setting where adversarial perspectives scrutinize all aspects of evidence, the objectivity of a radiological finding can provide absolute proof of abnormality or injury and a perspective from which clinical features can be understood by the court. For example, as shown in Figure 2.1, the clinical neuroimaging performed on the day of injury provides indisputable evidence of traumatic brain injury (TBI). The patient in Figure 2.1 sustained severe head trauma, including skull fractures and prolonged coma after an industrial fall of approximately 25 feet. The initial computed tomography (CT) scan objectively characterizes the acute injury; including skull fracture, right epidural hematoma, right-sided (coup) contusion and left-sided (contrecoup) contusion. The location of the scalp swelling and the skull fracture further establish the location and force of the impact.

As also shown in Figure 2.1, follow-up magnetic resonance (MR) imaging or MRI 20 months post-injury objectively shows the long-term consequences of the injury, including focal areas of tissue loss referred to as *encephalomalacia* due to the contusions and generalized loss of brain tissue resulting in diffuse brain atrophy. Correlation of the types and locations of brain abnormalities as demonstrated radiographically allows prediction of the neurological deficits and confirmation of cognitive and neuropsychological evaluations.

In disorders with acute onset, like head trauma or stroke, an initial CT scan, when available, is the most powerful method of showing the mechanism and the acuteness of the injury. In the case of head trauma, as shown in Figure 2.1, the presence of acute hemorrhage (white on CT scans) allows proof that the event in question, not some other event, caused the injury. Later examinations do not contain this information because the fractures heal, swelling resolves, blood is broken down and injured brain tissue is resorbed. The later scans, particularly MRI, show the final outcome of the head injury, effectively demonstrated by sequential MRI scans that show the loss of brain tissue. This is also true for stroke, or for tracking any type of lesion over time. In addition to the large lesions of head trauma, such as contusions, MRI can show shear lesions of gliosis (scarring) and focal deposits of hemosiderin (a blood breakdown product) as permanent markers of shearing trauma to the brain or prior hemorrhage. In the courtroom, the radiographic examinations

Neuroimaging in Forensic Psychiatry: From the Clinic to the Courtroom, First Edition. Edited by Joseph R. Simpson.

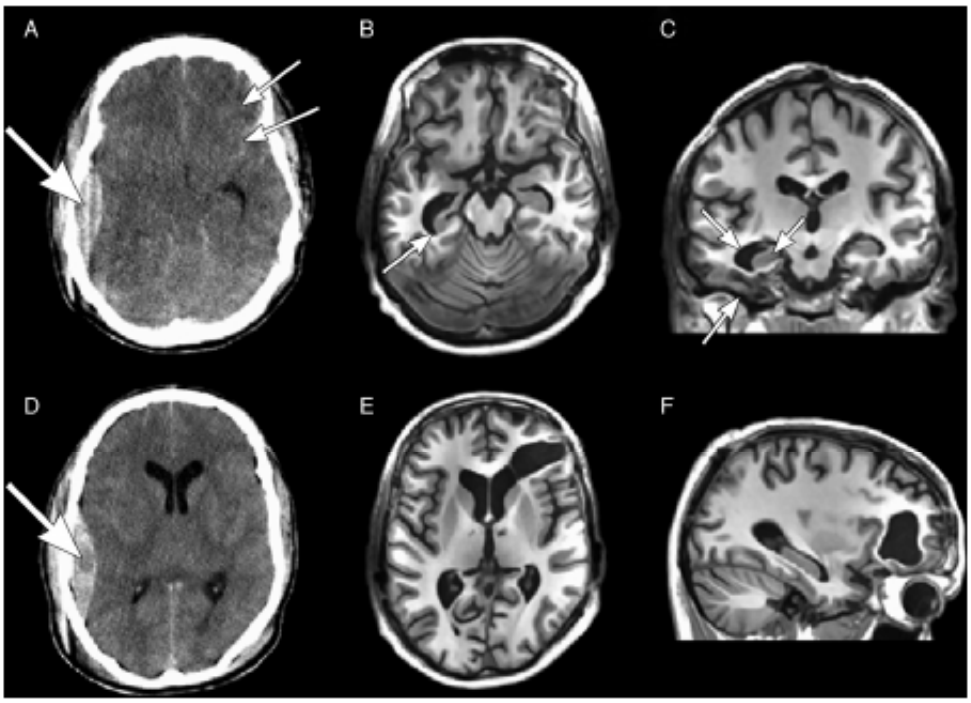

Figure 2.1 (A), (D) Day of injury axial CT scan showing an epidural hematoma (left arrow); (B), (E) follow-up MRI (20 months post-injury) at approximately the same level as the earlier CT, demonstrating significant structural and atrophic changes from the brain injury; (C) MRI coronal view depicting hippocampal atrophy and temporal horn dilation; (F) MRI sagittal view depicting a large cystic lesion in the frontal lobe and associated atrophic changes.

can demonstrate the immediate nature and severity of the injury as well as the long-term outcome. MRI methods also demonstrate generalized atrophic changes of the brain when present, important for assessing degenerative diseases where mental competency may be questioned. This chapter highlights some basic and advanced MRI methods, including objective techniques for demonstrating structural pathologies and functional relationships.

Conventional imaging, such as standard CT and MRI scans, as in Figure 2.1, show the qualitative effects of focal and diffuse brain damage, but do not address such questions as, 'How much tissue has been lost?' 'How has this brain changed?' 'How may these changes be quantified, and how do they relate to medical, neurobehavioral and neurocognitive outcome in someone with a neurological condition?' The conventional imaging report represents the radiologist's qualitative impression. As an adjunct to this qualitative evaluation of the scans, there are new and reliable quantitative methods that can also be applied to radiographic interpretations [1, 2, 3]. Quantitative analyses of neuroimaging findings provide additional objectivity to the qualitative radiological report.

Because many neurodevelopmental and neuropsychiatric disorders show no gross abnormalities on traditional CT or MRI scans, methods that measure brain structure and function are essential to the assessment of such conditions. Additionally, in progressive disorders, quantitative neuroimaging objectively documents the rate of atrophic changes over time, which relates to rates of cognitive decline. Objective standards and

normative comparisons applied to image analysis can now assess essentially all major brain regions of interest (ROI) with respect to morphology, volume, thickness, surface area, shape, contour, morphology and underlying biochemistry [4]. Function can also be inferred from MRI, where subtle differences in the blood oxygen level-dependent (BOLD) signal reflect hemodynamic responses in the brain to sensory, motor or cognitive stimuli. A directional diffusion-sensitive MRI technique called diffusion tensor imaging (DTI) permits an examination of neural connectivity. The integration of these neuroimaging techniques provides the clinician and the courtroom with objective information about brain structure and function.

Structural neuroimaging basics

An overview and historical context of diagnostic imaging is provided in Stimac [5]. As shown in Figure 2.1, gross anatomical information of the brain and skull can be identified by CT imaging; however, in comparison to MRI, CT provides limited contrast resolution (i.e. ability to distinguish structures of different composition). CT employs X-ray beam technology and computed image reconstruction to provide images based on the density of the structure in the brain. Because it is fast, easy to perform and effectively shows fractures, hemorrhage and mass effect, it is the preferred standard neuroimaging modality for any condition that requires emergent decision-making. As such, it is often the first neuroimaging assessment obtained, providing the initial diagnosis and baseline findings for follow-up (i.e., in Figure 2.1 compare the initial CT scan findings to the follow-up MRI shown in Figure 2.4). Most non-emergent clinical neuroimaging of the brain is done with MRI.

MR images of the brain are representations of the intensities of electromagnetic signals from hydrogen nuclei; a detailed understanding of the physics behind MRI is beyond the scope of this review [see 6, for a basic primer]. The MR signal is the result of a resonance interaction between hydrogen nuclei and externally applied magnetic fields spatially encoded to provide a mapping of the image area in two or three dimensions. The signal intensity depends on the density and the magnetic environment of the hydrogen nuclei (i.e., protons). The most important components of MRI are the protons, an external magnetic field, the interaction of the protons with the magnetic field and excitation of the protons by radiofrequency (RF) pulses.

The fundamental principle of clinical MRI is that the protons in the body (mostly from hydrogen), when placed in a strong magnetic field, respond to electromagnetic waves (radio waves, similar to those used in FM radio) by absorbing and then re-radiating these waves in accordance with the magnetic environment of the tissue. Thus, the re-radiated waves have a signal strength that characterizes the type of tissue. For example, structures of high water content, such as tumors, have longer-lasting signal strength than tightly structured tissues, such as fat. The source locations for the waves are specified by varying the magnetic field slightly, giving each volume element of the brain ('voxel') a unique frequency. The receiver can then assign the location of each signal to a specific location. The result is a map, or series of slices of the brain, in which the different tissues are characterized by their signal intensity, appearing brighter or darker on the images.

The use of innovative methods for varying the magnetic field strength, the delays between the sending and receiving of the radio waves and the acquisition and display of the signal intensity allow a wide range of images to be produced, some of which demonstrate

Table 2.1 MRI appearance of commonly scanned tissues

Tissue	T1-weighted	T2-weighted	Proton density-weighted
Gray matter	Gray	Light gray	Light gray
White matter	White	Dark gray	Gray
CSF or water	Black	White	Dark gray
Fat	White	Black	Black
Air	Black	Black	Black
Bone or calcification	Black	Black	Black
Edema	Gray	White	White
Demyelination or gliosis	Gray	White	White
Ferritin deposits (e.g., in basal ganglia)	Dark gray	Black	Black
Calcium bound to protein	White	Dark gray	Dark gray
Proteinaceous fluid	White	Variable	Variable

Note: On fast spin echo (FSE) sequences (a faster variant of the SE sequence), fat appears bright in T2- and proton density- weighted images.

anatomy to best advantage, some of which demonstrate pathology. For example, the behavior of the protons is characterized by two time constants, called T1 and T2. T1 reflects the rapidity with which protons become re-aligned with the magnetic field after an RF pulse. Scans that are T1-weighted tend to show greater detail but less contrast between structures; these images are therefore optimum for showing anatomy or for demonstrating the effects of intravenous paramagnetic contrast enhancement. T2 reflects the decay of in-phase precession (desynchronization or 'dephasing') of protons after the pulse. Scans that are T2-weighted generally show normal structures as having an intermediate (gray) intensity, while fluid and many pathologic abnormalities appear with high intensity (white). These images provide excellent contrast between normal and abnormal structures and are, therefore, used for identifying pathology. Sequences that provide an average of T1- and T2-weighting are called *proton density sequences*. The appearance (brightness) on the various sequences can be used to characterize the tissue. Common appearances of typical tissues are listed in Table 2.1 and demonstrated in Figure 2.2.

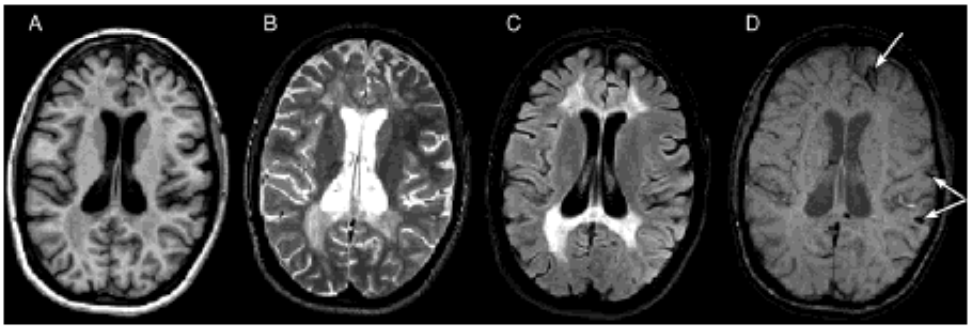

Figure 2.2 As shown in Table 2.1, each imaging sequence shows unique findings of normal and abnormal brain tissue signal intensity at the same level in the brain in the same individual. (A) T1; (B) T2; (C) FLAIR; (D) SWI. This patient had sustained a severe TBI with each sequence demonstrating unique morphological and pathological findings. For example, note that the T1 and SWI sequences do not demonstrate the white matter changes shown in the T2 and FLAIR. In contrast, note how large the frontal hemorrhagic lesion is in the SWI sequence shown in (D); while detected in the other imaging sequences, the size is substantially smaller.

Many types of MRI sequences have been developed and employed to provide additional characterization of abnormalities. For example, a sequence that uses subtle changes in magnetic field strength, called *gradient echo* or GRE, allows excellent image detail in short imaging times and has the added advantage of being sensitive to the presence of a blood breakdown product called hemosiderin. A susceptibility-weighted imaging sequence or SWI is particularly sensitive in detecting microhemorrhages, as shown in Figure 2.2. Fluid attenuated inversion recovery (FLAIR; see Figure 2.2) and short T1 inversion recovery (STIR) sequences use an inversion recovery process to obtain a much greater contrast between normal tissue and abnormal tissue as compared with standard spin-echo T2 images. Diffusion sequences use the motion of free water in the brain to identify ischemia and to measure the integrity of white matter tracts in the brain. The use of intravenously injected paramagnetic contrast material allows demonstration of abnormal blood flow, inflammation and infection. Other sequences demonstrate the flow of blood in the vessels to show vascular anatomy and oxygen uptake.

The magnetic field strength of MRI scanners is typically between 0.5 and 3.0 Tesla (T). Today, most brain imaging is performed at 1.5 T. New, higher strength 3.0 T scanners provide increased spatial resolution and allow performance of many types of functional imaging, including diffusion tensor imaging (DTI). Many of the advanced techniques discussed below, including DTI, MR spectroscopy (MRS) and functional MRI, provide better results with or require the higher field strength. Experimental use above 3.0 T is providing even more exquisite anatomical and pathological detail about the brain [7].

Quantitative MRI (qMRI)

Some of the pathology shown in the case presented in Figure 2.1 was obvious, like the increased size of the temporal horns of the lateral ventricle or the appearance of smaller hippocampal size for a young adult. These are clinical indicators of damage to the temporal lobe and its structures, but how significant is that damage? Quantitative MRI or qMRI provides a method to compare a given patient's MRI data to a normative sample and answer that question.

When it comes to neural tissue, there is a biological fact that is fortunate for imaging purposes. At the gross anatomical level there are just two tissue types – white and gray matter – and within the cavities of the brain, cerebrospinal fluid (CSF). Obviously, there are blood vessels embedded within the brain parenchyma as well, which can be separately analyzed by a variety of radiological techniques, but for the purposes of standard image quantification it is typically restricted to just white matter, gray matter and CSF volume and/or morphology.

Figure 2.3 shows a normal T1 anatomical image and the normal appearance of the hippocampus along with the normal slit-like appearance of the temporal horn (compare this to the patient shown in Figure 2.1). The T1 image clearly shows that each tissue type – gray matter and white matter along with the spaces filled with CSF – has specific signal intensity as displayed on a gray scale. The differences in pixel intensities provide the basis for 'segmentation' of all gray, white and CSF identified, as shown in Figure 2.3(B), where gray matter is now colorized as red, white matter as white and CSF as black (see color plate section). Next, in what used to require a hand-tracing method, computer programs 'classify' the different structures and ROIs by their gray, white and CSF boundaries [8] (see Figure 2.3(C)). Once classified by knowing the dimensions of an ROI, the volume, shape and a variety of other measures may be quantified, including the thickness of cortical regions.

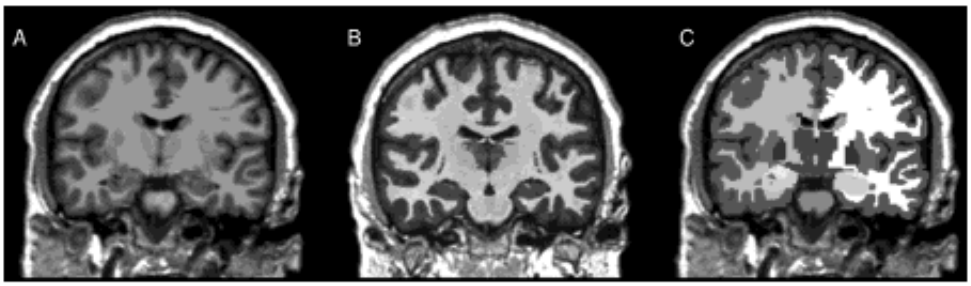

Figure 2.3 Segmentation and classification. (A) T1 image; (B) segmented image where red reflects gray matter, white is white matter and black represents CSF; (C) classified image where each color designates a different structure or region of interest. Please see Plate 2 for color figure.

Returning to the patient who sustained a severe TBI shown in Figure 2.1, the degree of hippocampal atrophy and temporal horn dilation (and any other ROI) can now be quantified and compared to standardized normative databases [1]. Figure 2.4 shows this patient's classified image, where the hippocampus is colorized as yellow and the temporal horn in aquamarine (see color plate section). With this method, gray matter abnormalities are identified, as shown in red. Hippocampal volumetrics show that it is below the 10th percentile for age, with temporal horn dilation about the 99th percentile for age. These values provide objective quantification of the structural damage to the temporal lobe. Figure 2.4 also shows how quantitative MRI neuroimaging findings can be shown in 3D, which assists in straightforward identification of abnormalities and their relationship to overall brain anatomy.

The most common qMRI value is a volume, but other measurements including surface area, contour and shape analyses, as well as cortical thickness can be performed [9]. Another technique referred to as *voxel-based morphometry* [10] uses digital MRI data that are 'smoothed' within a uniform space so that all brains have the same X-Y-Z dimensions. Each pixel is then classified as being white matter, gray matter or CSF; then determining the relative concentration of different pixel types within a specified voxel allows the computation of 'voxel-by-voxel' white, gray and CSF comparison. Volume changes in pixel density as determined by the VBM technique can objectively demonstrate where differences occur in a brain compared to a reference sample [11]. Strangman *et al.* [12] have shown how utilizing some of these qMRI-identified abnormalities predicts neuropsychological outcome in the damaged brain.

Functional MRI applications to understanding brain activation and function

Over the last two decades, functional MRI (fMRI) has emerged as the dominant technique for functional brain mapping in laboratory research settings [for excellent primers, see 13, 14]. Functional MRI is based on the physiological fact that when neural activity increases in a brain region, blood flow to that region increases. The increased regional flow results in a localized surplus of oxyhemoglobin relative to deoxyhemoglobin. These two molecules have different magnetic properties. The change in the oxyhemoglobin:deoxyhemoglobin ratio resulting from regional neural activation yields the blood oxygen level dependent, or BOLD, signal. Adapting fMRI for use outside of the laboratory requires special

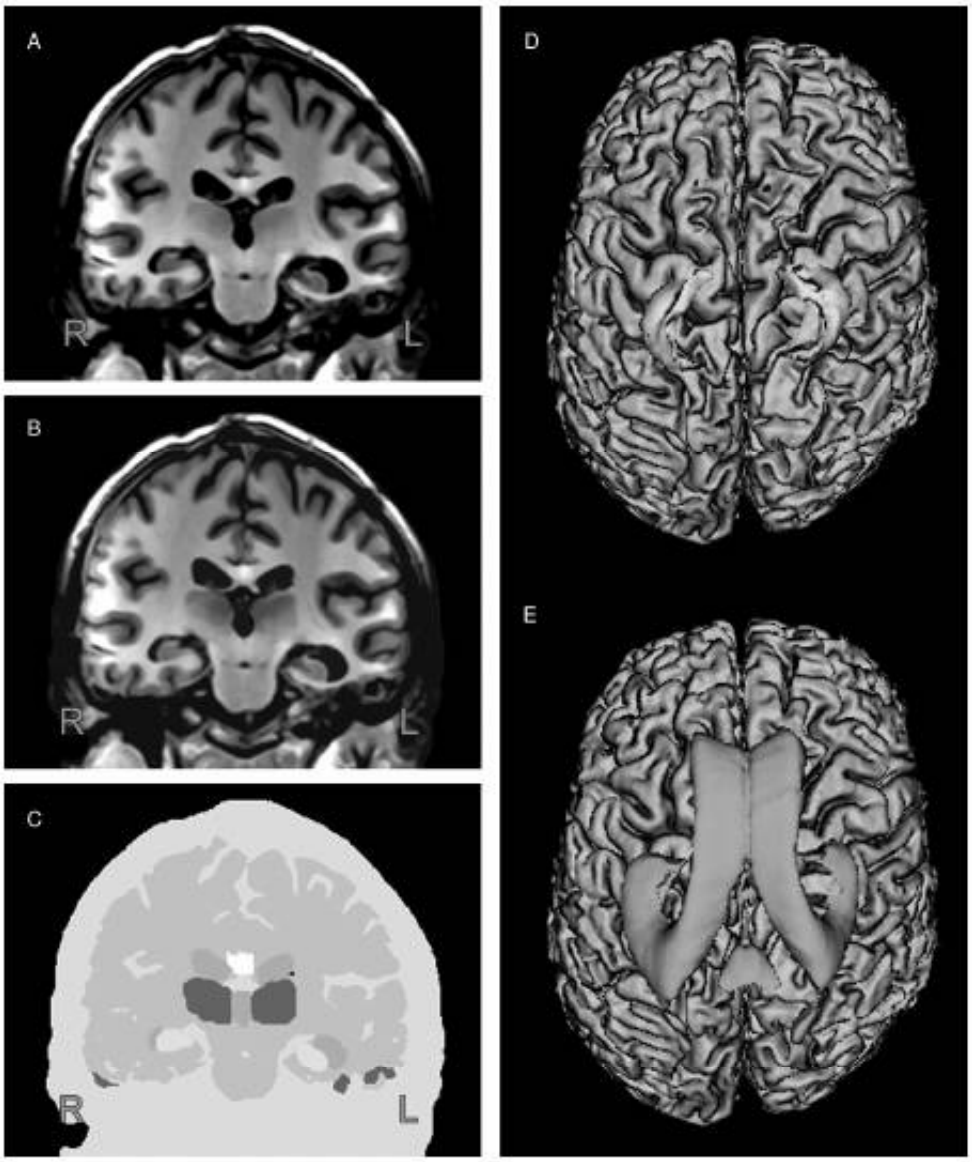

Figure 2.4 Classification of temporal horn (aquamarine) and hippocampus (yellow) for image quantification. This is the same patient as shown in Figure 2.1. Please see Plate 3 for color figure.

considerations [15], especially in a forensic setting [16–18]. This section focuses on the unique problems that have been addressed in bringing fMRI technology from the laboratory into clinical and forensic applications.

Foremost among the challenges of clinical fMRI is that in typical research applications, fMRI relies on the increased statistical power that comes from averaging data from multiple subjects. By necessity, however, most clinical and forensic applications of fMRI require analysis of activations in a single individual. One reason research-based

fMRI studies typically use group averaging is to increase signal-to-noise values. BOLD-identified differences require detection of small signal fluctuations that arise from subtle changes in magnetic field homogeneity – often resulting in less than 1% of total signal change in an image point across the course of a scan. Nonetheless, with careful attention to details of physics, neuro- and vascular physiology, cognitive theory, psychological processes and basic experimental design, it is becoming more common to develop fMRI paradigms that produce clean and reliable activation patterns from single individuals.

For example, the Trail Making Test (TMT), Part B, a classic neuropsychological test which is presumed to assess executive functioning, mental flexibility, psychomotor speed and other lower- and higher-level cognitive processes, and is easily administered in paper-and-pencil test format [19], can be adapted for fMRI assessment. The basic cognitive task is to have the subject connect numbers and letters in sequence (i.e., 1 – A – 2 – B – 3 – C and so on until 13 numbers and 12 letters have been connected). This may initially appear easy, but from a cognitive and neural-network standpoint the task involves complex and bi-hemispheric integration of neural function to complete. However, without *in vivo* documentation of which brain regions are activated, clinical neuropsychology may only infer what brain regions participate in a given task. When the task is performed during fMRI, the actual brain regions that participate in the task can be viewed, as shown in Figure 2.5. In

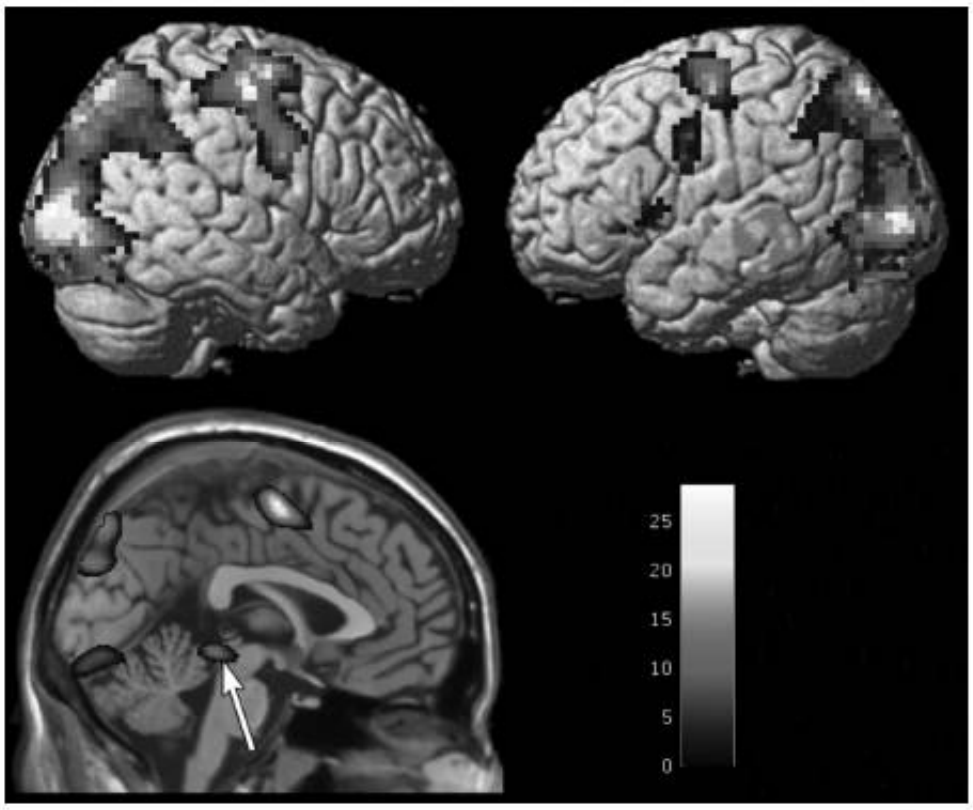

Figure 2.5 Activation from a single-subject performing an fMRI adaptation of the Trail Making Test-B. Color bar represents *t*-values derived from analysis of covariance (ANCOVA) model of task activation compared to an implicit baseline.

this normal subject, robust fMRI activation is elicited where group studies of many subjects performing this task show similar activation patterns; hence, in this case what is observed would be classified as a 'normal' activation pattern for the TMT neurocognitive probe in this subject [20].

From an interpretative perspective, the parietal activations observed in Figure 2.5 reflect the sum total activations likely related to the brain's attentional and working memory networks essential to TMT performance. These regions also overlap with spatial processing centers, which integrate with visual centers as well as motor output. Since the task involves elements of language processing and a motor response, greater left frontal activation in the region involving Broca's area reflects engagement of language and probably motor planning. However, these findings also demonstrate some of the expected subtle specificity of activation that can be achieved with current fMRI technology. For example, note the tectal activation (indicated by the arrow). The superior colliculus in the upper tectum is a small subcortical structure, which has a well-established function in visual search and visual attention, and would be expected to participate in a task like TMT-B. This illustrates a high degree of precision that can be obtained in single-subject scanning, and then compared to normative group data.

While the example offered in Figure 2.5 is specific to activation during TMT performance, demonstrating neural regions that participate in that task, essentially any cognitive process where discrete cognitive or behavioral performance can be measured can be adapted for fMRI. These cognitive, neural fMRI probes can be adapted to include tasks of memory function, visual discrimination and reaction time, spatial processing, auditory and language processing, somatosensory processing and executive functioning [21–23]. Additionally, fMRI can be integrated with standard structural MRI to show whether damaged areas activate normally or not [24]. In such an application the traditional methods of MRI analysis are first applied showing whatever abnormalities may be identified.

For example, the patient shown in Figure 2.6 sustained massive temporal lobe damage to the lateral surface of both temporal lobes as a result of a fall of approximately 15 feet, evidenced by the pronounced encephalomalacia. This patient underwent bilateral craniotomies and excision of macerated temporal lobe tissue from a combination of skull fractures, contusions and hematomas. Obviously, the lateral surface of the temporal lobes was massively damaged. The clinical question was whether medial temporal lobe activation still occurred in response to a memory probe, especially at the level of the hippocampus. As can be seen in Figure 2.6, using an fMRI-based memory probe known to activate the hippocampus, medial temporal lobe activation occurred despite the extensive damage to the lateral aspects of the temporal lobe. Such findings helped in understanding how to approach rehabilitation care and treatment of the patient and indicated that memory retraining might be a viable approach even in a patient with this extensive level of damage [24].

The precision of fMRI to demonstrate cognitive correlates like lateralization of language function has become an important development in pre-surgical mapping. This has been by far the largest effort to perfect single-subject fMRI analysis, where testing protocols, particularly for motor functions that relate to laterality, have been refined to the highest levels of precision currently available [25]. However, the goals of clinical and forensic fMRI are likely different from those of pre-surgical planning. Specifically, the value of fMRI sought by most clinical and forensic applications is its potential to assess levels of cognitive and brain functioning in an individual, with respect to what is expected in the absence of pathology. This method becomes particularly valuable to the extent that it can

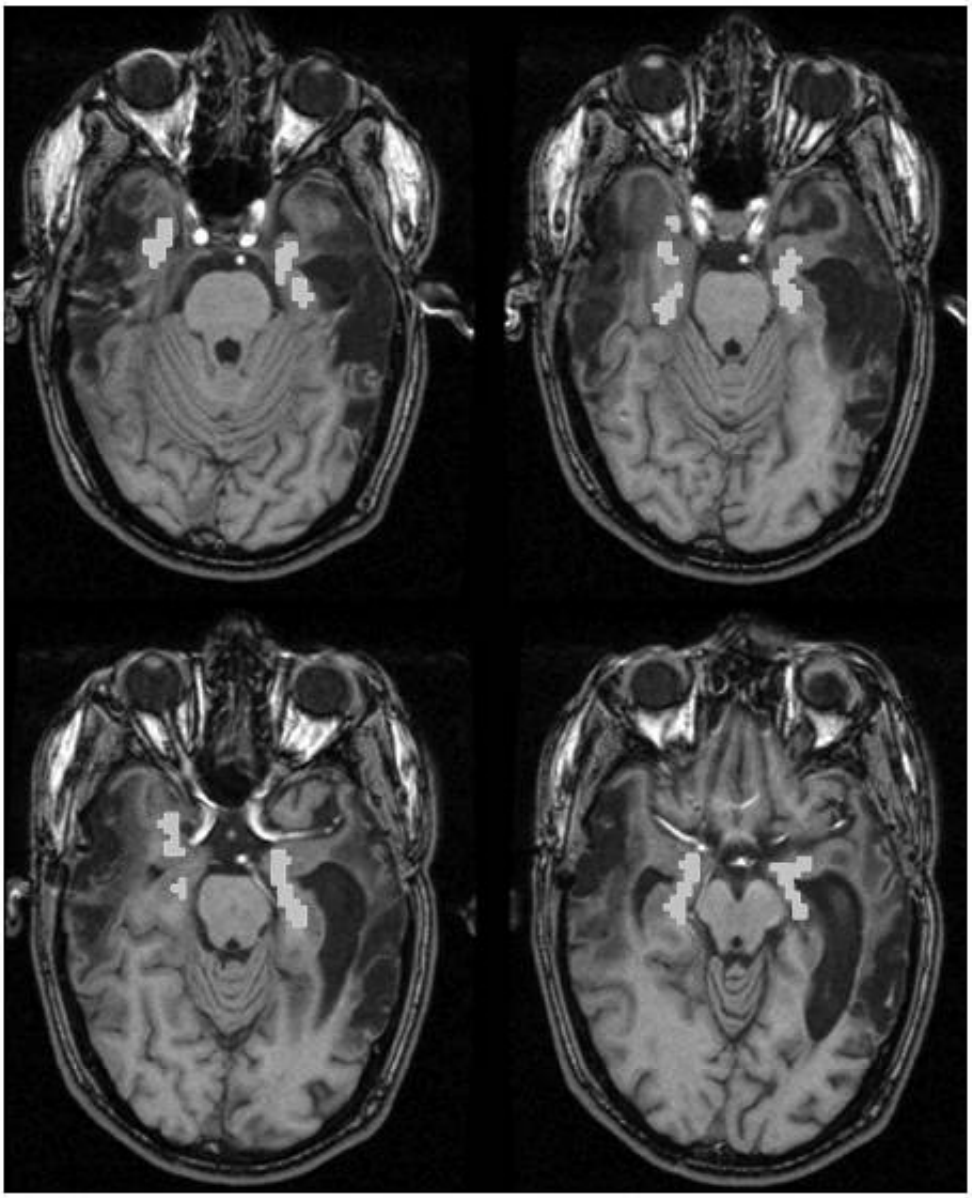

Figure 2.6 Activation overlain on structural scans, where normal activation is present on an fMRI adaptation of a face memory encoding test (f-FMT), despite obvious and severe medial temporal lobe damage.

identify abnormality (in function) that might otherwise go undetected using standard imaging and/or neuropsychological testing approaches. This, in turn, highlights the importance of using normative data when assessing and interpreting fMRI findings [13, 26].

The case presented in Figure 2.7 shows how fMRI can be used to probe functional neural correlates in a case where standard structural MRI revealed no abnormalities. The fMRI findings were from a National Guard soldier who served in Iraq and returned to the U.S.

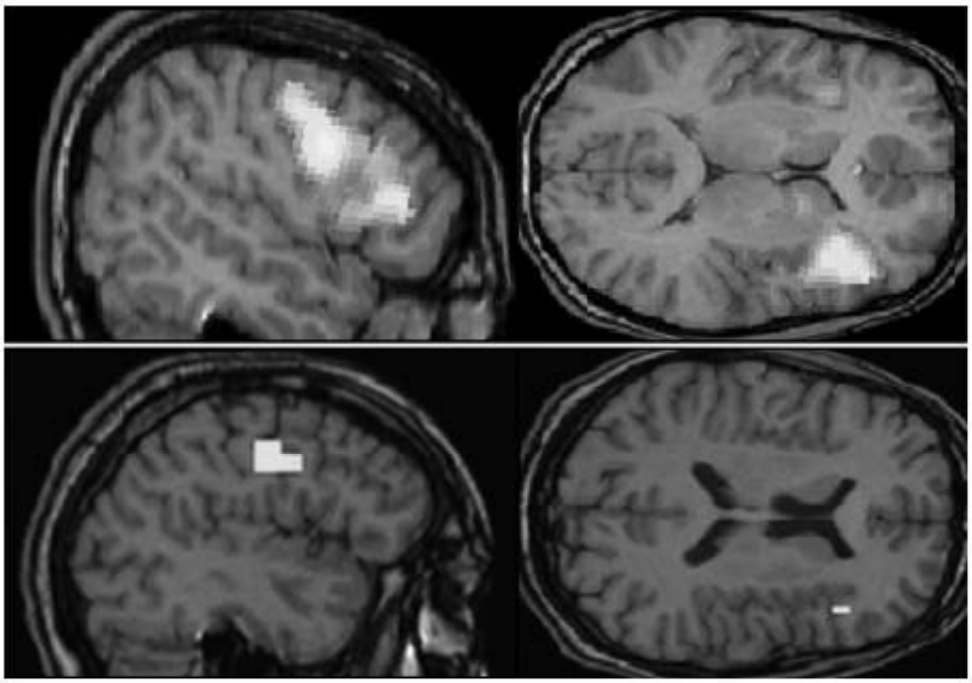

Figure 2.7 Activation from a control subject (upper row) and Patient 1 (lower row) on an fMRI adaptation of the verbal fluency task (f-VFT). Scans are shown in radiological convention (L = R).

after experiencing three consecutive road-side IED blasts within one month. In his initial assessment for post-concussive and post-traumatic stress disorder (PTSD), both of which were confirmed, he underwent conventional MRI, which was unremarkable. Clinically, he also had developed stuttering, which, given the initial negative MRI findings and presence of PTSD, was assumed to be a byproduct of anxiety. However, since one effect of sustaining a mild traumatic brain injury may be reduced verbal fluency [27], the patient was scanned using a battery of fMRI adaptations of common neuropsychological exams, including verbal fluency testing [22]. As shown in Figure 2.7, this patient's activation images deviate markedly from a composite normative sample. There are now a number of fMRI studies showing abnormal activation patterns in patients with normal-appearing structural imaging who have blast-related head injuries [28, 29] or PTSD [30]. The fMRI activation differences do not necessarily prove underlying pathology, but clearly demonstrate that neural activation is different than the norm.

Magnetoencephalography (MEG) has also been integrated with structural and functional MRI to show regions of activation and cortical engagement during cognitive tasks [31], but is still very much an experimental procedure. Similarly, various electroencephalographic (EEG) techniques can also be integrated with structural and functional MRI [32], but these too are mostly experimental methods at this time.

Diffusion tensor imaging

Another major development in MRI methods is diffusion tensor imaging (DTI). DTI measures directionality of water diffusion, from which additional inferences can be made about

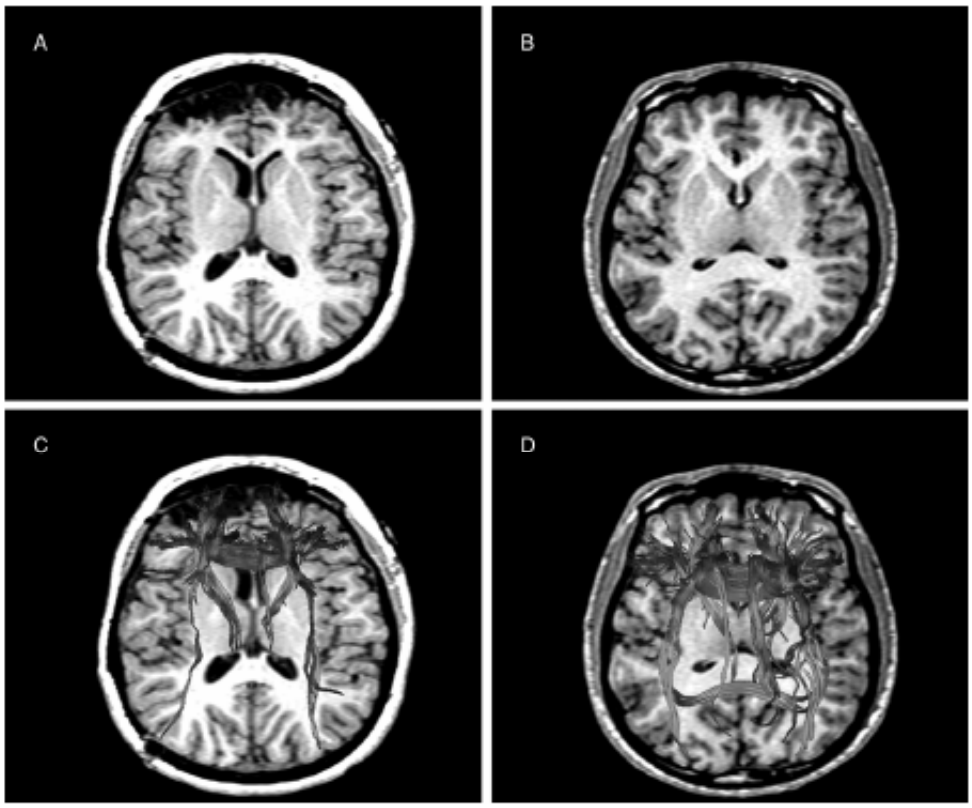

Figure 2.8 DTI demonstration of loss of tracts in a child with brain injury where conventional MRI shows massive frontal encephalomalacia as depicted in (A) (dark signal involving both frontal poles) as compared to the age-matched control in (B). (C) shows the effects of the frontal damage on the tracts associated with frontal projections, which are markedly reduced in (C) compared to the control in (D). Please see Plate 4 for color figure.

the integrity of brain parenchyma, especially white matter [33–35]. As shown in Figure 2.8, there are DTI techniques that provide additional information about pathway damage and disconnection in the brain that simply cannot be visualized using conventional MRI. In the brain-injured child with massive frontal damage shown in Figure 2.8, the true effects of the frontal pathology may only be fully appreciated by understanding how the focal damage disrupts and disconnects neural pathways into and out of the frontal lobe, as distinctly shown by DTI that demonstrates the overall reduction and loss of neural tracts.

Conclusion

The objectivity of various neuroimaging methods discussed in this chapter provides a wealth of information about the structure and function of the human brain that may have particular value in a forensic setting. Combining standard clinical interpretative findings of MRI with objective volumetric and morphometric analyses, including the assessment of microstructural integrity as shown by DTI, provides for a range of approaches for

evaluating pathology. This, combined with the emergence of fMRI to address clinical questions [36, 37], heralds an increasing role for neuroimaging in the forensic arena.

Acknowledgment

The technical assistance of Tracy Abildskov in illustration preparation is gratefully acknowledged.

References

1. Brewer, J.B. (2009) Fully-automated volumetric MRI with normative ranges: Translation to clinical practice. *Behav. Neurol.*, **21**, 21–28.
2. Deoni, S.C. (2011) Magnetic resonance relaxation and quantitative measurement in the brain. *Methods Mol. Biol.*, **711**, 65–108.
3. Schnack, H.G., van Haren, N.E., Brouwer, R.M., van Baal, G.C., Picchioni, M., Weisbrod, M. *et al.* (2010) Mapping reliability in multicenter MRI: Voxel-based morphometry and cortical thickness. *Hum. Brain Mapp.*, **31**, 1967–1982.
4. Pearlson, G.D. and Calhoun, V. (2007) Structural and functional magnetic resonance imaging in psychiatric disorders. *Can. J. Psychiatry*, **52**, 158–166.
5. Stimac, G.K. (1992) *Introduction to Diagnostic Imaging*. Philadelphia: W.B. Saunders.
6. Hunt, R.H. and Thomas, K.M. (2008) Magnetic resonance imaging methods in developmental science: A primer. *Dev. Psychopathol.*, **20**, 1029–1051.
7. Tallantyre, E.C., Morgan, P.S., Dixon, J.E., Al-Radaideh, A., Brookes, M.J., Morris, P.G. *et al.* (2010) 3 Tesla and 7 Tesla MRI of multiple sclerosis cortical lesions. *J. Magn. Reson. Imaging*, **32**, 971–977.
8. Bigler, E.D., Abildskov, T.J., Wilde, E.A., McCauley, S.R., Li, X., Merkley, T.L. *et al.* (2010) Diffuse damage in pediatric traumatic brain injury: A comparison of automated versus operator-controlled quantification methods. *Neuroimage*, **50**, 1017–1026.
9. Destrieux, C., Fischl, B., Dale, A. and Halgren, E. (2010) Automatic parcellation of human cortical gyri and sulci using standard anatomical nomenclature. *Neuroimage*, **53**, 1–15.
10. Ashburner, J. (2009) Computational anatomy with the SPM software. *Magn. Reson. Imaging*, **27**, 1163–1174.
11. Ridgway, G.R., Henley, S.M., Rohrer, J.D., Scahill, R.I., Warren, J.D. and Fox, N.C. (2008) Ten simple rules for reporting voxel-based morphometry studies. *Neuroimage*, **40**, 1429–1435.
12. Strangman, G.E., O'Neil-Pirozzi, T.M., Supelana, C., Goldstein, R., Katz, D.I. and Glenn, M.B. (2010) Regional brain morphometry predicts memory rehabilitation outcome after traumatic brain injury. *Front Hum. Neurosci.*, **4**, 182.
13. Brown, G.G., Perthen, J.E., Liu, T.T. and Buxton, R.B. (2007) A primer on functional magnetic resonance imaging. *Neuropsychol. Rev.*, **17**, 107–125.
14. Huettel, S., Song, A. and McCarthy, G. (2004) *Functional Magnetic Resonance Imaging*. Sunderland, MA: Sinauer Associates.
15. Kozel, F.A. and Trivedi, M.H. (2008) Developing a neuropsychiatric functional brain imaging test. *Neurocase*, **14**, 54–58.
16. Dressing, H., Sartorius, A. and Meyer-Lindenberg, A. (2008) Implications of fMRI and genetics for the law and the routine practice of forensic psychiatry. *Neurocase*, **14**, 7–14.
17. Kulich, R., Maciewicz, R. and Scrivani, S.J. (2009) Functional magnetic resonance imaging (FMRI) and expert testimony. *Pain Med.*, **10**, 373–380.
18. Patel, P., Meltzer, C.C., Mayberg, H.S. and Levine, K. (2007) The role of imaging in United States courtrooms. *Neuroimaging Clin. N. Am.*, **17**, 557–567.
19. Lezak, M.D., Howieson, D.B. and Loring, D.W. (2004) *Neuropsychological Assessment*. New York: Oxford University Press.
20. Allen, M.D., Owens, T.E., Fong, A.K. and Richards, D.R. (2011) A functional neuroimaging analysis of the Trail Making Test-B: Implications for clinical application. *Behav. Neurol.*, **24**, 159–171.

21. Allen, M.D., Hedges, D.W., Farrer, T.J. and Larson, M.J. (2011) Assessment of brain activity during memory encoding in a narcolepsy patient on and off modafinil using normative fMRI data. *Neurocase*, in press.
22. Allen, M.D. and Fong, A.K. (2008) Clinical application of standardized cognitive assessment using fMRI. I. Matrix reasoning. *Behav. Neurol.*, **20**, 127–140.
23. Allen, M.D. and Fong, A.K. (2008) Clinical application of standardized cognitive assessment using fMRI. II. Verbal fluency. *Behav. Neurol.*, **20**, 141–152.
24. Strangman, G.E., O'Neil-Pirozzi, T.M., Goldstein, R., Kelkar, K., Katz, D.I., Burke, D. *et al.* (2008) Prediction of memory rehabilitation outcomes in traumatic brain injury by using functional magnetic resonance imaging. *Arch. Phys. Med. Rehabil.*, **89**, 974–981.
25. Pillai, J.J. (2010) The evolution of clinical functional imaging during the past 2 decades and its current impact on neurosurgical planning. *AJNR Am. J. Neuroradiol.*, **31**, 219–225.
26. Rosen, A.C. and Gur, R.C. (2002) Ethical considerations for neuropsychologists as functional magnetic imagers. *Brain Cogn.*, **50**, 469–481.
27. Strong, C.A., Tiesma, D. and Donders, J. (2011) Criterion Validity of the Delis–Kaplan Executive Function System (D-KEFS) Fluency Subtests After Traumatic Brain Injury. *J. Int. Neuropsychol. Soc.*, **17**, 230–237.
28. Matthews, S.C., Strigo, I.A., Simmons, A.N., O'Connell, R.M., Reinhardt, L.E. and Moseley, S.A. (2011) A multimodal imaging study in U.S. veterans of Operations Iraqi and Enduring Freedom with and without major depression after blast-related concussion. *Neuroimage*, **54**(Suppl 1), S69–75.
29. Van Boven, R.W., Harrington, G.S., Hackney, D.B., Ebel, A., Gauger, G., Bremner, J.D. *et al.* (2009) Advances in neuroimaging of traumatic brain injury and posttraumatic stress disorder. *J. Rehabil. Res. Dev.*, **46**, 717–757.
30. Eckart, C., Stoppel, C., Kaufmann, J., Tempelmann, C., Hinrichs, H., Elbert, T. *et al.* (2011) Structural alterations in lateral prefrontal, parietal and posterior midline regions of men with chronic posttraumatic stress disorder. *J. Psychiatry Neurosci.*, **36**, 176–186.
31. Lewine, J.D., Davis, J.T., Bigler, E.D., Thoma, R., Hill, D., Funke, M. *et al.* (2007) Objective documentation of traumatic brain injury subsequent to mild head trauma: Multimodal brain imaging with MEG, SPECT, and MRI. *J. Head Trauma Rehabil.*, **22**, 141–155.
32. Driver, J., Blankenburg, F., Bestmann, S. and Ruff, C.C. (2010) New approaches to the study of human brain networks underlying spatial attention and related processes. *Exp. Brain Res.*, **206**, 153–162.
33. Chanraud, S., Zahr, N., Sullivan, E.V. and Pfefferbaum, A. (2010) MR diffusion tensor imaging: A window into white matter integrity of the working brain. *Neuropsychol. Rev.*, **20**, 209–225.
34. DaSilva, A.F., Tuch, D.S., Wiegell, M.R. and Hadjikhani, N. (2003) A primer on diffusion tensor imaging of anatomical substructures. *Neurosurg. Focus*, **15**, E4.
35. Feldman, H.M., Yeatman, J.D., Lee, E.S., Barde, L.H. and Gaman-Bean, S. (2010) Diffusion tensor imaging: A review for pediatric researchers and clinicians. *J. Dev. Behav. Pediatr.*, **31**, 346–356.
36. Friston, K.J. (2009) Modalities, modes, and models in functional neuroimaging. *Science*, **326**, 399–403.
37. Atri, A., O'Brien, J.L., Sreenivasan, A., Rastegar, S., Salisbury, S., Deluca, A.N. *et al.* (2011) Test-retest reliability of memory task functional magnetic resonance imaging in Alzheimer disease clinical trials. *Arch. Neurol.*, **68**, 599–606.

Part II

Clinical and Research Findings